Energy Scavenging for Body Sensor Networks

Elizabeth K. Reilly
University of California Berkeley
2111 Etcheverry Hall
Berkeley, CA 94720
001-510-301-3931
beth@kingkong.me.berkeley.edu

Paul K. Wright
University of California Berkeley
2117 Etcheverry Hall
Berkeley, CA 94720
001-510-643-6546
pwright@me.berkeley.edu

ABSTRACT

For small, inexpensive, ubiquitous wireless sensors to be realized, all constituents of the device, including the power source, must be directly integratable. For long term application the device must be capable of scavenging power from its surrounding environment. An apparent solution lies in conversion of mechanical energy to electrical output via the growth and direct integration of piezoelectric thin films unimorphs with the wireless electronics. Current devices are limited by both their design and material selection. This paper will address optimizing the design of microscale devices by showing how the device strains under input vibration are directly proportional to its power output, and by proposing some designs which increase the strain distribution over more of the device volume. Finite element modeling (ANSYS®) was used to determine the strain distribution in a cantilever, modified cantilever, trapezoid, and spiral shaped piezoelectric microscale energy scavenging system. The devices have been fabricated and initial results are presented.

Categories and Subject Descriptors

B.7.1 [**Integrated Circuits**]: Types and Design Styles - *advanced technologies*

General Terms

Performance, Design, Reliability, Experimentation

Keywords

Sensor networks, energy scavenging

1. INTRODUCTION

Wireless sensor networks is viewed by many observers as the 'third wave of computing' (after the main frame and personal computing).[1,2,3,4] Recently, a combination of technology trends, that is, cheaper and lower power electronics resulting from the continuation of Moore's law, represent major progress in ad-hoc wireless connectivity. The availability of mesoscale (on the order of several centimeters) peripheral devices such as sensors, energy sources and antennas has made this third wave of computing a possibility for medical applications, smart buildings, agriculture, and environmental monitoring in nature.[5] However, the power supply to the wireless nodes and related devices remains a challenge (< 2-3 years of life of 2 AA batteries for Zigbee nodes) and low power radio design is key.

BODYNETS 2007, June 11-13, Florence, Italy

DOI 10.4108/bodynets.2007.169

(a)

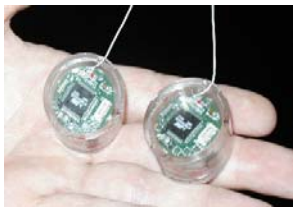

(b)

Figure 1. a) Wireless sensor "nodes" or "motes," b) practical size of 2 cm^3

Energy scavenging offers an alternative for power supply and a number of approaches have been studied over the past years. Stordeur and Stark[6] have demonstrated a thermoelectric device that can produce 15 μW of power from a 10 °C temperature differential. Shenck and Paradiso[7] have built shoe inserts capable of generating 8.4 mW of power under normal walking conditions. Amirtharajah and Chandrakasan[8] have demonstrated an electromagnetic vibration-to-electricity converter with a 4x4x10 cm^3 volume that produces 400 μW of power (or 2.5 μW/cm^3). Much research has, of course, focused on solar (photovoltaic) power.[9] Single crystal solar (photovoltaic) cells offer efficiencies of about 15% for inexpensive commercially available cells and over 40% for high-end research cells. Thin-film polycrystalline cells, which exhibit efficiencies of 10 – 13%, are also available. Thin-film amorphous silicon solar (photovoltaic) cells have a lower efficiency ranging from 8 – 10%, but are well suited for indoor applications because their

spectral response closely matches that of fluorescent white light. CdTe cells have a wide spectral response, and so perform well either indoors or outdoors. In the absence of available light sources mechanical energy scavenging has become a viable option. Vibration generators based on electromagnetic[10,11,12], electrostatic[13], and piezoelectric[14] conversion have been suggested in the literature. The body represents a natural source of mechanical energy through its motion during day to day activities. The relatively low frequency and high amplitudes of these vibrations make vibrational energy scavenging and attractive option for powering body centered wireless networks.

It is our opinion that piezoelectric vibration-to-electricity converters offer great potential at the meso-scale level, and piezoelectric generators can outperform electromagnetic generators at low frequency. At high frequencies, above several thousand hertz, the internal capacitance of the piezoelectric tends to reduce the amount of real power that can be drawn from the device. This suggests that piezoelectric devices are better suited to low frequency human body powered applications. Roundy[11] tabulated the vibration characteristics of many household appliances, manufacturing equipment, and HVAC ducts showing that the dominant frequency of most commonly occurring vibration sources is between 50 and 300 Hz.

The integration of piezoelectrics on silicon has been a widely explored topic. In recent years the growth of epitaxial ferroelectric films on silicon have paved the way for the integration of these films in microelectromechanical systems. The fabrication procedure of the thin film form of most piezoelectrics (sol-gel, sputtering, etc.) employs a high temperature growth environment or annealing step which results in large scale residual stresses in the film making them virtually impossible to use. For applications that require large piezoelectric coefficients, such as vibrational energy scavenging, it is essential that the films be grown epitaxially to ensure high piezoelectric activity. Piezoelectric materials are perfect candidates for vibrational energy scavenging as they can efficiently convert mechanical strain to an electrical charge without any additional power[11]. This paper will explore the use of thin film piezoelectric microelectromechanical systems as vibrational energy scavenging systems.

2. CONVERSION DESIGN

The energy conversion from mechanical vibration into electrical power can be described using the elements of linear spring mass system with electrical and mechanical damping terms (Eq. 1).

$$m\ddot{z} + (b_e + b_m)\dot{z} + kz = -m\ddot{y} \qquad (1)$$

Where z is the lumped mass displacement, y the base displacement, m the lumped mass, k the spring constant, b_m the mechanical damping coefficient, and b_e is the electrical damping coefficient.

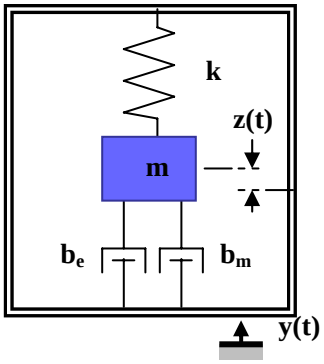

Figure 2. Schematic of generic vibration converter

Using this simple model the power output of this system at resonance is shown in Eq. 2 and is independent of transduction mechanism (i. e. electrostatic, electromagnetic, or piezoelectric.)

$$P = \frac{m\xi_e A^2}{4\omega(\xi_e + \xi_m)} \qquad (2)$$

Where $b=2m\xi\omega_n$ and represents the relative damping ratio, A the acceleration input of the input vibration, and ω the operation frequency. The system should be designed so that it mechanically resonates at a frequency tuned with ambient vibration. A study done by Roundy et al.[11] shows that most of the available environmental vibrations are at lower frequencies. Therefore in order to maximize the power output the energy scavenging device should resonate at a frequency lower that 1 kHz.

2.1 Transduction Mechanisms and Power Density

The fundamental parameters limiting the generator output are its proof mass m and maximum internal displacement Z_l, and the source motion amplitude Y_0 and frequency ω.[22] From these we can derive the maximum power from basic principles. If we assume harmonic source motion, the maximum acceleration $a_{max} = \omega^2 Y_0$. The maximum damping force by which energy can be extracted is equal to the inertial force on the proof mass, ma_{max} (if greater, the mass will not move). If energy is extracted in both directions, the internal motion amplitude $Z_o = Z_l$, (giving the maximum travel range of $2Z_l$) we derive a total energy per cycle of $4Z_l ma_{max} = 4Z_l m\,\omega^2 Y_0$. To convert this to power we simply divide by the excitation period $2\pi/\omega$, giving:

$$P_{max} = 2Y_0 Z_l \omega^3 m / \pi \qquad (3)$$

We can then define a normalized power $P_n = P/P_{max}$ as a measure of how close the performance of a specific device comes to the optimum level.

In the ideal case, the parasitic damping would be zero, and maximum power is then obtained by setting the electrical

damping factor ζ_e to the level that allows the mass to move over the entire internal range, but without hitting the end-stops, i.e. $Z_0=Z_l$.[23] However, in some cases the maximum damping force of the transducer is insufficient to achieve this, and therefore the device cannot operate in a resonant mode. In cases where the parasitic damping factor ζ_p is not negligible, maximum power will inevitably be reduced, but the optimum ζ_e will still be that which gives $Z_0=Z_l$, unless this requires $\zeta_e < \zeta_p$, in which case $\zeta_e = \zeta_p$ should be chosen if possible.

2.2 Analytical Solution

The analytical solution for power generation from an independent piezoelectric cantilever assuming capacitive circuit coupling has been calculated elsewhere[22]. Assuming an epitaxial PZT piezoelectric coefficient, cantilever dimensions with a calculated resonance frequency of 950 Hz, typical (not optimized) elastic/piezoelectric thickness and ratio, and simple capacitive circuit power coupling, we calculate that each microcantilever beam can generate approximately 5.5 nW (Figure 3). Considering cantilever dimensions, we arrive at an areal power density of 5 $\mu W/cm^2$, and an area projected volume power density of 80 $\mu W/cm^2$.

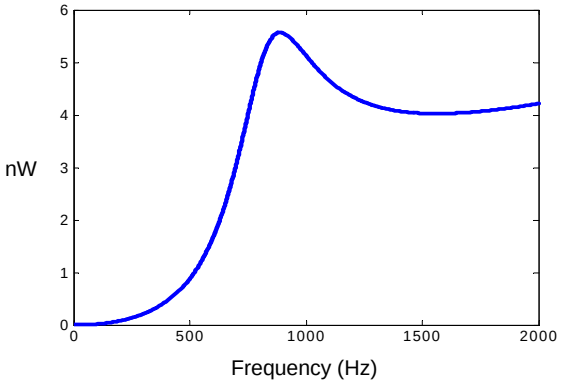

Figure 3. Estimated power output per 800 μm cantilever beam

Although this calculated power density is at the threshold of the estimated required power for most low power radios, this model *may* be on the lower estimation side and is located in its entirety elsewhere[27]. Tapered cantilever shapes would increase the area strained under excitation and may easily be fabricated to increase the generated power. Also, with slightly more elaborate, but still standard, microfabrication processes a proof mass was added to the end of the cantilever beams to increase deflection, reduce the resonant frequency, and increase the power output.

3. MECHANICAL DESIGN

The constitutive equations for thin film piezoelectric cantilever beams are expressed in reduced tensor form below:

$$S_1^p = s_{11}^p T_1 - d_{31} E_3 \quad (4)$$

$$-D_3^p = d_{31} T_1^p - \varepsilon_{33}^T E_3 \quad (5)$$

Where S^x_i is the strain, s_{ij} is the elastic compliance, T^x_i is the stress, d_{ij} is the piezoelectric coupling coefficient, E_i is the electric field, D_i is the dielectric displacement, and ε_{ij} is the relative electrical permittivity. The superscript indicates the effected element (E= elastic layer, P= piezoelectric layer, T= constant stress) and the subscript indicates the direction.

When the beam is strained anti-parallel to the polarization in the lower, piezoelectric element the element creates an electric field across the thickness of the beam (Fig. 4).

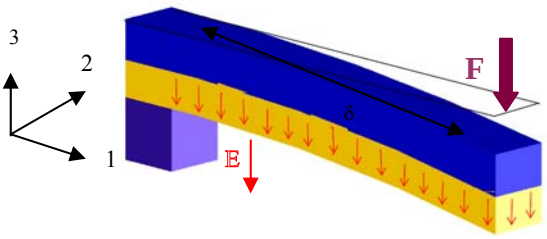

Figure 4. Schematic of piezoelectric cantilever under input acceleration

Ideally, the upper non-piezoelectric element will not interact with the induced field or resist deformation of the active layer under input mechanical deformation, but will serve as an electrode to harness the surface charge created. At equilibrium it may be assumed the there is no movement of the individual layers at the interface, i.e., the layers are tightly joined. Using these assumptions the total electric field created under input vibration is:

$$E_3 = \frac{1}{d_{31}}\left[\frac{F^p s_{11}^p}{w h_p} + \frac{F^e s_{11}^e}{w h_e} + \frac{h_p M^p}{2E^p I^p} + \frac{h_e M^e}{2E^e I^e}\right] \quad (6)$$

Where F is the applied forced due to vibration, M is the applied moment, I is the moment of inertia, h is the thickness of the element, and w is the width of the beam.

Several simplifications can be made due to the geometry of the system. First, the film layers are sufficiently thin so that they have a common radius of curvature.

$$R = \frac{M^p}{E^p I^p} = \frac{M^e}{E^e I^e} \quad (7)$$

Therefore for a cantilever beam:

$$M^e = M^p \left(\frac{h_e}{h_p}\right)^3 \left(\frac{s_{11}^P}{s_{11}^e}\right) \quad (8)$$

Secondly at equilibrium there is no net displacement in the 1-direction and the moments about the free end sum to zero.

$$M^p + M^e = F\left(\frac{h_p}{2} + \frac{h_e}{2}\right) \quad (9)$$

Plugging Eq. 6, 8, and 9 into Eq. 4 gives the expression for electric field (E_3) as a result of input strain (S_1^P).

$$E_3 = \frac{S_1^p B}{(1 - d_{31} B)} \quad (10)$$

$$B = \frac{4 s^p s^e h_E h_p^3 + 4 s_{11}^p s_{11}^e h_e^3 h_p + (s_{11}^p)^2 h_p^4 + 6 s_{11}^p s_{11}^e h_e^2 h_p^2}{4 s_{11}^e h_p^3 + s_{11}^p h_e^3 - 6 s_{11}^e z_p (h_p h_e + h_p^2) + 3 s_{11}^e h_p^2} \quad (11)$$

$$where \ (\quad 0 \le z_p \le h_p)$$

The output voltage is calculated by Eq. 12 and is used estimating the power output (Eq. 13).

$$V_3 = \int_0^{h_p} E_3 dz_p = \int_0^{h_p} \frac{S_1^P B}{(1 - d_{31} B)} dz_p \quad (12)$$

The maximum voltage occurs at the surfaces of the piezoelectric (z_p= 0, h_p). The voltage calculated above is through a cross section of the beam and must be integrated along the entire width and length of the beam to achieve the overall voltage produced. However, as shown in the next section, the strain concentration varies along the length of most geometries and therefore is not a trivial calculation and will be further explored in subsequent work.

$$P = \frac{V_{\max}^2}{R} \quad (13)$$

$$R_{opt} = \frac{1}{\omega C_o} \quad (14)$$

$$\therefore P = \frac{1}{\omega C_o} \int_0^{h_p} E dz_p \quad (15)$$

Typical capacitance values for a MEMS piezoelectric cantilever range from 0.1- 1 nF [25]. The power equation may be expanded over the entire geometry to determine the output of the entire device. However the simplified above analysis demonstrates the direct correlation to output power to the strain felt by the piezoelectric. From this result it is clear that a design should optimally distributes the strain due to vibration along the totally volume of the piezoelectric.

3.1 Finite Element Analysis

ANSYS® finite element software was used to model the strain concentrations in various geometries in order to determine alternative design configurations that result in superior distribution of strain under input vibrations. Designs explored include a modified cantilever (Fig. 4a, b), a trapezoid (Fig. 5), and a spiral (Fig. 6). The geometries were chosen to keep the resonant frequencies between 1000-10,000 Hz, which is higher than what are available from ambient vibrations but are lower than most MEMS devices. These devices may harness the subsequent nodal frequencies of most environments rather than the just the first. The first nodal resonant frequencies of the geometries are located in Table 1.

Table 1. Resonant Frequency

Geometry	Resonant Frequency (Hz)
Cantilever	1000
Modified Cantilever	1113
Trapezoid	5583
Spiral	6247

The frequencies tend to increase as the geometry becomes more complex. The resonant frequencies may be reduced through the application of a proof mass and changing the cross section (length, width) of the shapes. For modeling purposes the thicknesses of the various film layers were kept constant (total thickness 1.4 μm) and the density of PZT used was 7800 g/cm^3. The strain was determined by applying acceleration typical of those found in the residential environments, 2.25 m/s^2.

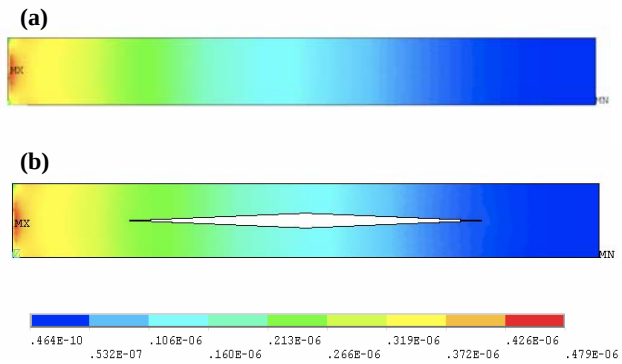

Figure 5. Finite element analysis of a) cantilever, b) modified cantilever design

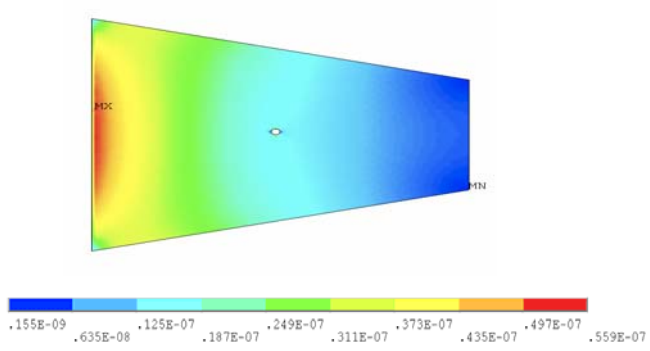

Figure 6. Finite element analysis of trapezoid design

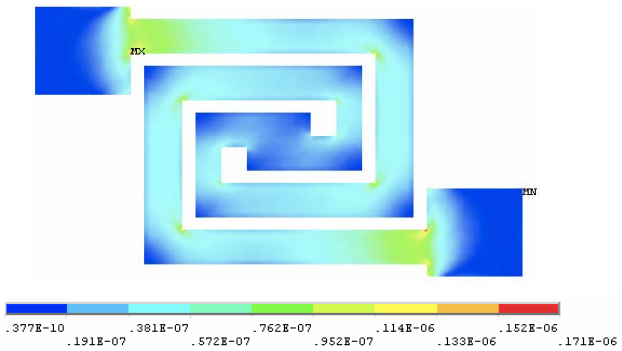

Figure 7. Finite element analysis of spiral design

The strain in the structures was compared by calculating the percentage of the geometry that underwent at least 20% of the maximum strain present in each of the structures under input acceleration. Table 2 compares the percent increase in strain over the original cantilever for different geometries.

Table 2. Geometry strain results and percent increase

Geometry	Percent of Area Strained (%)	Percent Increase (%)
Cantilever	40.4	0
Modified Cantilever	50.2	29.2
Trapezoid	55.6	37.7
Spiral	74.5	87.0

4. EXPERIMENTAL

Although many piezoelectric materials exist and are commercially available as thin films (thickness on the order of 1 micron), few of them exhibit large enough piezoelectric coefficients to generate appreciable voltage while under strain. The $Pb(Zr,Ti)O_3$ (PZT) family of piezoelectrics in general have large piezoelectric coefficients and can be grown epitaxially with careful selection of growth substrate and electrodes (typically oxide electrodes, such as $SrRuO_3$ (SRO) demonstrate usable conductivities when grown in thicknesses ≥ 50 nm). Epitaxial, or pseudo-single crystal, thin films are attractive because the piezoelectric coefficients, mechanical constants, and dielectric properties of the films can be an order of magnitude higher than polycrystalline films of the same composition.

The PZT ($PbZr_{0.47}Ti_{0.53}O_3$) film was grown on a Si/STO substrate via pulsed laser deposition.[8] Pulsed laser deposition was chosen for its ability to rapidly produce quality films. The quality of the piezoelectric films was determined through measurement of piezoelectric coefficient and remnant polarization. The d_{33} was determined using piezoforce microscopy and the results are located in Figure 8. It can be seen that the d_{33} value of the film is approximately 160 pm/V which approaches the bulk value and is vastly superior to those the films grown on Pt electrodes. The polarization hysteresis curve identifies the saturation polarization and remnant polarization as 58 and 42 $\mu C/cm^2$ respectively. These values continue to increase as the film fabrication optimized.

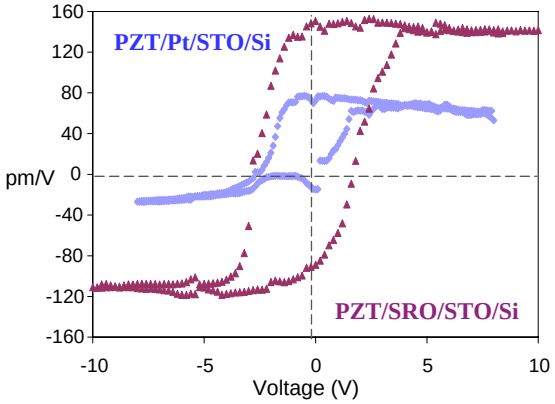

Figure 8. Piezoelectric coefficients for various film compositions

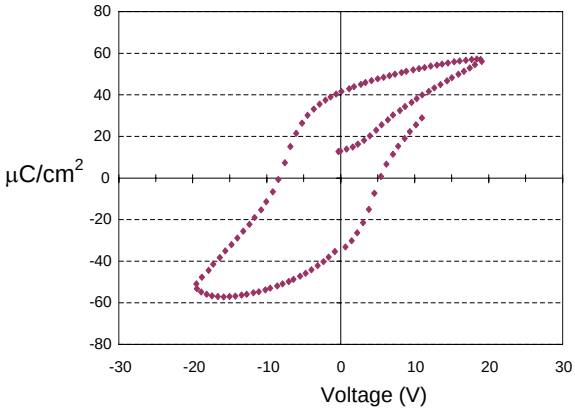

Figure 9. Polarization hysteresis loop

It should be noted the fabrication processes used to apply surface electrode causes a significant amount of damage to the surface of the film, as seen by the roundness of the hysteresis curve, therefore care must be taken while fabricating the device structures. Recent studies by Beneyad et al. show the fabrication of epitaxial PMN-PT with thin film piezoelectric coefficients in the range of 500 pm/V which mark a vast improvement of previously classes of piezoelectric materials.[32] Future fabrication attempts will include films of this stoichiometry.

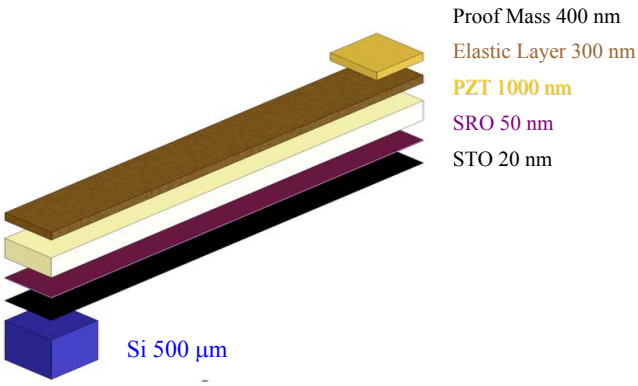

Figure 10. Configuration of thin film layers

The metallic layer is deposited using electron beam and thermal evaporation, and the device is then released from the substrate using xenon difluoride (XeF_2) gaseous etch. Because significant residual stresses were present in the film, neutral ion bombardment was used to balance the residual stresses of the film with application of an induced compressive stress layer[28-30]. Figures 11, 12, and 13 show scanning electron microscope photographs of the modified cantilever, trapezoid, and spiral films, respectively, fabricated for this study.

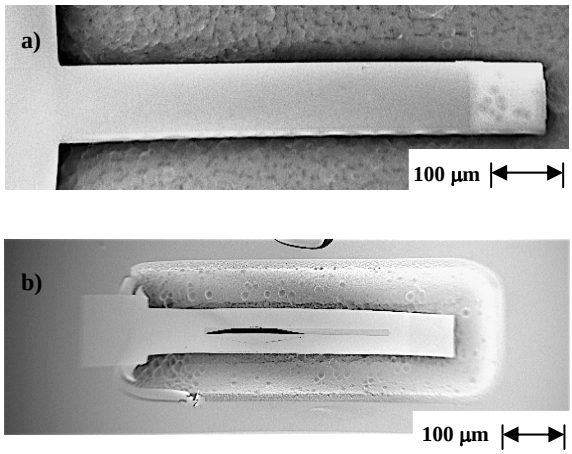

Figure 11. SEM photograph of a) cantilever, b) modified cantilever

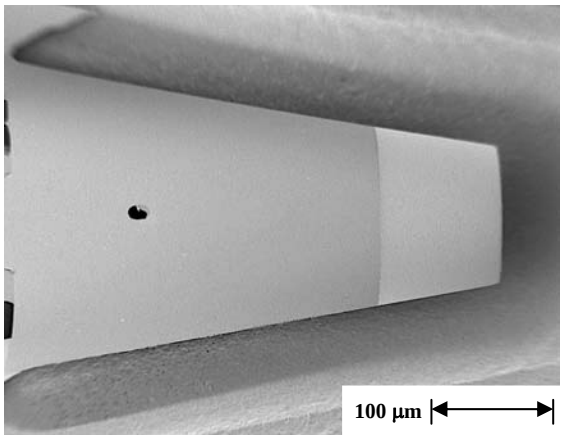

Figure 12. SEM photograph of trapezoid

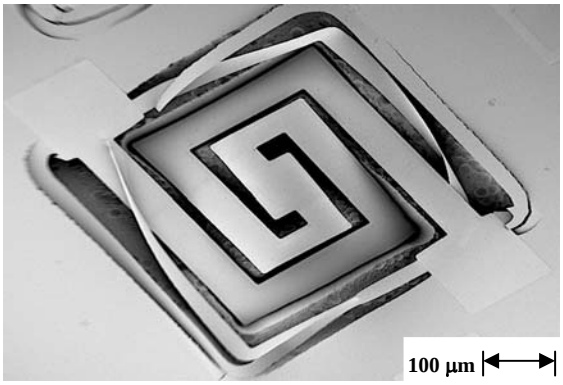

Figure 13. SEM micrograph of spiral

5. CONCLUSIONS

Microscale vibrational energy scavenging has gained popularity in recent years due the advancement in microfabrication techniques and ability to grow high quality piezoelectric films on silicon. Design of these devices becomes critical due to the small power density inherent in these devices. Maximizing the functionality of these devices using the restricted dimensions of a MEMS system creates a challenging problem. Geometries which demonstrate distributed strain concentrations over the entire device will markedly improve the power output. The modified cantilever, trapezoid, and spiral configuration all represent improvements in that they make use of between 50 – 75 % of the available piezoelectric versus the standard cantilever which only uses about 40%.

Thin film PZT has been grown epitaxially on silicon with a limited number of oxide buffer layers. The film shows good polarization and switching capabilities. The residual stress that commonly plagues MEMS devices has been compensated for using a combination of metallic layers and careful processing techniques. Preliminary power modeling shows a minimum

power density of 80 $\mu W/cm^3$, approaching the power requirement for most low power radios. Initial testing indicates the reduction of the resonant frequency with application of the proof mass.

6. ACKNOWLEDGMENTS

This work was performed in close collaboration with Professors Eric Yeatman and Paul Mitcheson of Imperial College London and R. Ramesh of University of California Berkeley.

Special thanks to Eric Carleton, Lindsay Miller, and Florin Zavialish. This work is a result of the generous funding of the Luce Foundation, Berkeley ITRI fellowship, and the California Energy Commission.

7. REFERENCES

[1] Birnbaum, J., www.hpl.hp.com/speeches/pervasive.html

[2] Weiser, M., The Computer for the 21st Century, *Scientific American,* 165, 3, (September 1991), 94-104. Reprinted in *IEEE Pervasive Computing* (March 2003), 19-25.

[3] Stanford, V., Using Pervasive Computing to Deliver Elder Care, *IEEE Pervasive Computing: Mobile and Ubiquitous Systems,* 1, 1, (January-March 2002), 10-13.

[4] Basten, T., Geilen, M., and de Groot, H., Ambient Intelligence: Impact on Embedded System Design, (2003), Kluwer Academic Publishers. 1-348, ISBN Number 1-4020-7668-1.

[5] Bulkeley, W., Wireless's New Hookup, *The Wall Street Journal*, Thursday February 24, 2005, Section BI Marketplace, 1.

[6] Stordeur, M., Stark, I., Low Power Thermoelectric Generator – self-sufficient energy supply for micro systems, *16th Int. Conf. on Therm*, (1997), 575-7.

[7] Shenck, N. S., Paradiso, J. A., 2001. Energy Scavenging with Shoe-Mounted Piezoelectrics, *IEEE Micro*, 21 (2001) 30-41.

[8] Amirtharajah, R., Chandrakasan, A.P., Self-Powered Signal Processing Using Vibration-Based Power Generation, *IEEE JSSC*, *33*, 5, (2002), 687-695.

[9] Randall, J.F. *On ambient energy sources for powering indoor electronic devices* Ph.D. thesis Ecole Polytechnique Federale de Lausanne, Switzerland May 2003.

[10] Roundy, S., Otis, B., Chee, Y-H., Rabaey, J., and Wright, P.K., A 1.9 GHz Transmit Beacon using Environmentally Scavenged Energy, *ISPLED*, Seoul, Korea, August 25-27, 2003.

[11] Roundy, S., Wright, P., and Rabaey, J., A study of low level vibrations as a power source for wireless sensor nodes, *Comput. Commun.*, *26*, (2003), 1131-1144.

[12] Shearwood, C., Yates, R.B., Development of an electromagnetic micro-generator, *Electronics Letters*, *33*, 22, IEE, 23, Oct. 1997, 1883-1884.

[13] Meninger, S., Mur-Miranda, J.O., Amirtharajah, R., Chandrakasan, A.P., and Lang, J.H., Vibration-to-Electric Energy Conversion. *IEEE Trans. VLSI Syst., 9* (2001) 64-76.

[14] Roundy S., and Wright, P., A Piezoelectric Vibration based Generator for Wireless Electronics, *Smart Materials and Structures, 13*, (2004), 1131-1142.

[15] Bates, J., Dudney, N., Neudecker, B., Ueda, A., Evans, C., Thin-film lithium and lithium-ion batteries, *Solid State Ionics*, *135,* (2000), 33 – 45.

[16] Harb, J., LaFollette, R., Selfridge, R., Howell, L. Microbatteries for self-sustained hybrid micropower supplies, *Journal of Power Sources*, *104,* 1, (2002), 46 – 51.

[17] Dewan, C., Teeters, D., Vanadia xerogel nanocathodes used in lithium microbatteries, *Journal of Power Sources*, *119* (2003), 310 – 315.

[18] Jeon. et. al. MEMS power generator with transverse mode thin film PZT, *Sens. and Actuators A. 122*, (2005), 16-22.

[19] S. J. Kim, K.-I. Hong, and D.-K. Choi, Fabrication and Characterization of Pb(Zr, Ti)O_3 Microcantilever for Resonance Sensors, *Jpn. J. Appl. Phys. 42*, 3, (2003) 1275-1478.

[20] Glenn-Jones, P., Beeby, S., and White, N.,Towards a piezoelectric vibration-powered microgenerator, *IEE Proc. Sci., Meas. Technol., 148*, (2001), 69-72.

[21] Kymissis, J. et. al., Parasitic power harvesting is in shoes, *Proceedings of the Second IEEE International Conference on Wearable Computing ISWC*, Pittsburg, PA, USA 1998.

[22] Mitcheson, P., Reilly, E., Wright, P., and Yeatman, E., Transduction Mechanisms and Power Density for MEMS Inertial Energy Scavengers, *Proceeding of the Fourth International Conference on PowerMEMS*, Berkeley, CA, USA, 2006, *in press.*

[23] Mitcheson, P, Green, T, Yeatman, E, and Holmes, A., Architectures for vibration-driven micropower generators, *Microelectromechanical Systems, Journal of*, *13*, (2004), 429-440.

[24] Guyomar, D., Badel, A., Lefeuvre, E., and Richard, C., Toward energy harvesting using active materials and conversion improvement by nonlinear processing, *IEEE Transactions on Ultrasonics Ferroelectrics and Frequency Control*, *52*, (2005), 584-595.

[25] Reilly, E., Miller, L., and Wright, P., Optimizing On-Chip Piezoelectric Energy Scavenging for Integration of Medical Sensors with Low-Power Wireless Networks, *Wearable and Implantable Body Sensor Networks*, 2006. BSN 2006.

[26] Reilly, E., and Wright, P., Thin Film Piezoelectric Energy Scavenging Systems for an On-Chip Power Supply", *Proceeding of the Fourth International Conference on Power MEMS*, Berkeley, CA, USA, 2006, *in press.*

[27] Reilly, E. *Design and Fabrication of a Thin Film Piezoelectric Vibrational Energy Scavenging System*, Masters Thesis, University of California Berkeley, Berkeley CA, 2004.

[28] Bifano T., Johnson, H., Bierden, P., and Mali, R., Elimination of Stress-Induced Curvature in Thin-Film Structures, *J. Microelectromech. Sys.*, *11*, 5, (2002) 592-597.

[29] Huand, S., Li, B., and Zhang, X., Elimination of stress-induced curvature in microcantilever infrared focal plane arrays, *Sens. and Actuat. A*, in press

[30] Bifano, T., Johnson, H., Bierden, P., and Mali, R., Elimination of Stress-Induced Curvature in Thin-Film Structures, *J. Microelectromech. Sys.*, *11*, 5, (2002) 592-597.

[31] Benyad, G. Sebald, L. Lebrun, B. Guiffard, S. Pruvost, D. Guyomar, and L. Beylat, "Segregation study and segregation modeling of Ti in $Pb[(Mg_{1/3}Nb_{2/3})_{0.6}Ti_{0.4}]O_3$ single crystal growth by Bridgman method," *Mater. Res. Bull.,* in press